HISTOGRAM FILTER FOR ATTITUDE DETERMINATION OF SMALL ASTEROID LANDER

M. Schlotterer, R. Findlay, T.-M. Ho, L. Witte, C. Ziach.

German Aerospace Center, Institute of Space Systems

Robert-Hooke-Str. 7, 28359 Bremen, Germany, markus.schlotterer@dlr.de

ABSTRACT

The Mobile Asteroid Surface Scout (MASCOT) is a small landing package build by the German Aerospace Center (DLR) jointly with the French Space Agency (CNES). MASCOT will fly onboard the Japanese space probe Hayabusa-II, built by the Japan Aerospace Exploration Agency (JAXA) and is scheduled to be launched in late 2014 on a 5-year sample return mission to the Near-Earth Asteroid 1999 JU$_3$. The lander is equipped with four science instruments which will take detailed close-up pictures and make a variety of in-situ measurements. MASCOT has a cubic shape roughly $29\,cm \times 27.5\,cm \times 20\,cm$ and weighs about $10\,kg$. An internal mechanism with an eccentric tappet can be used to reorient MASCOT if needed and relocate to a different site to increase its investigation area.

After the arrival and a characterization of the asteroid, MASCOT will be dropped from the Hayabusa-II mothership and will land passively on the asteroid surface. Before starting science measurements MASCOT must lie on the correct side. The attitude determination system consists of 2 types of sensors: solar cell based sun sensors on each side of MASCOT as well as 5 optical proximity sensors (OPS). The latter consists of an LED and a photodiode which can detect the reflected LED light when MASCOT is in proximity to the surface.

A histogram filter is used for attitude determination and multi sensor data fusion. It is a bayesian filter used to estimate states which can be divided in a finite number of possible values. This is useful for MASCOT since all that is needed is an estimation of the side on which it is lying.

This paper focuses on the attitude determination system of MASCOT. It describes the attitude determination sensors and the details of the filter algorithm. It also presents simulation results for system verification, as well as planned Monte-Carlo simulation and Hardware-in-the-Loop tests.

1. INTRODUCTION

For the navigation of spacecraft algorithms are needed to estimate states from the measurement of different sensors. One widely used class of algorithms are Kalman Filters, especially Extended Kalman Filters (EKF) and more and more also Unscented Kalman Filters (UKF) [4]. All of them have in common that they require Gaussian noise sources, a more or less linear system and an exact knowledge of the systems dynamics and measurement model. For robotic missions, especially exploration missions this is not always given: due to contact dynamics the system model is highly nonlinear and even not very well known in many cases. A common answer to this are Particle Filters or Gaussian Sum Filters with the drawback of a complex implementation, high computational load, big tuning effort and without guarantee of convergence in any case. For some cases also the not so well known Histogram Filter is a good choice.

The Mobile Asteroid Surface Scout (MASCOT) is such a case. It will fly onboard the Japanese space probe Hayabusa-II to the Near-Earth Asteroid 1999 JU$_3$ and will be dropped after arrival to land passively on the asteroid surface. The task of its GNC system is to determine the side on which MASCOT is lying. The fact that these 6 possible sides are a discrete state of the system with a finite number of states makes the Histogram Filter a preferred choice.

This paper starts with a description of the MASCOT mission and lander. An extra section is dedicated to the MASCOT GNC System, showing the system concept and architecture as well as the used sensors. The paper gives a short theoretical introduction in Bayesian Filters in general with a special focus on the Histogram Filter. It will also be shown how this type of estimation algorithm can be adapted for the MASCOT GNC System. The last section presents the test and verification methods to show that the proposed algorithm is suitable for the given requirements. For the software simulation also simulation results will be shown.

2. MASCOT

The exploration of minor bodies in the last few decades extended from flybys like Deep Space 1, orbiting (e.g. NEAR Shoemaker or Dawn) to sample return like Hayabusa. Future sample return missions, such as Hayabusa-2 and OSIRIS-REx are currently planned.

The link between remote sensing, in-situ and sample return science can be achieved with multiple landings and in-situ measurements over a variety of asteroid terrains. An agile, lightweight, highly capable mobile platform is desirable.

The German Aerospace Center (DLR) is currently developing in collaboration with CNES and ISAS/JSPEC/JAXA a lander (MASCOT) in the class of a nanosatellite for the Hayabusa-2 mission. With a total mass of $\sim$10 kg , MASCOT carries four scientific instruments: a camera (DLR), a hyperspectral microscopic imager (IAS), a magnetometer (TU Braunschweig) and a radiometer (DLR). The payload cumulatively weights $\sim$3 kg. Once landed in 2018/19 on the C-type asteroid, (162173) 1999 JU$_3$, the four instruments will study in-situ its surface morphology and geological setting, its regolith structure, texture and composition, the thermal and magnetic properties of the surface on 2-3 landing sites, enabled by MASCOT's ability to hop across the asteroid.

A. LANDER CONCEPT

The MASCOT bus has a total volume of about $0.3 \, \text{m} \times 0.3 \, \text{m} \times 0.2 \, \text{m}$. The structure is of lightweight carbon fiber sandwich framework supporting the payloads (P/L), a common electronic box, the passive thermal control surfaces and the antennae for communication during surface operation. To upright itself into correct instrument orientation and to perform relocation via hopping on the asteroid surface, MASCOT is equipped with a mobility mechanism and a suite of GNC sensors. Control, housekeeping, autonomy, data handling and local processing power are provided by a redundant on-board computer (OBC). Power is supplied by primary battery via a redundant power subsystem (PCDU). The design goal is to operate up to two asteroid days (one asteroid day is $\sim$7.5 h) on the surface. Communications to Earth is established via relay by the mothership. Due to the short duration of surface operations ($<$16 h), the amount of direct telemetry to and control commands from Earth is extremely limited, requiring almost complete autonomy of the lander. During cruise and the first phase of target reconnaissance, MASCOT is carried in a mechanical and electrical support structure (MESS) attached to the HY-2 spacecraft. Within this time MASCOT is mostly inactive; thermal control and power supply for in-cruise operations are provided by the mothership.

B. MISSION CONCEPT

The interplanetary cruise will take approximately 4 years, with MASCOT nominally off except for commissioning and periodic monitoring and calibration activities.
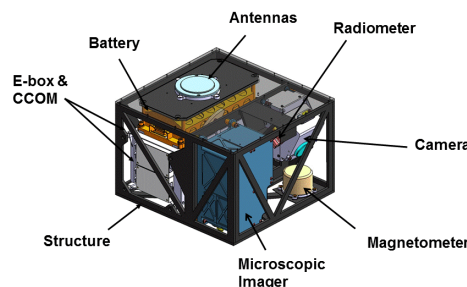

Fig. 1: CAD model of MASCOT incl. PL and S/S

After arrival at (162173) 1999 JU$_3$, Hayabusa-2 (HY-2) will first perform a global mapping in order to characterize the asteroid, and also to assist with landing site selection for it's sample return touchdown and MASCOT deployment.

With the landing site selected (based on local geology and thermal constraints), MASCOT will be released to the surface, either during a dedicated descent or during one of the sampling touchdown rehearsals. HY-2 will descend to the separation altitude of 100 m at which point MASCOT will get ejected via a spring mechanism. The lander will fall to the asteroid surface under the effects of the weak gravity field, before touch-down in an unknown orientation. The descent to the asteroid after ejection will take approximately 20 min, with communications to Hayabusa-2 maintained throughout. If possible, MASCOT will also take camera images of the asteroid during descent.

Once landed, the highest priority of MASCOT is to upright and perform the scientific measurements. After completion of the first science cycle, the lander will relocate and start the 2nd science cycle.

C. MASCOT GNC SYSTEM

The tasks of the MASCOT GNC system are the detection of the motion state of the lander as well as the estimation of the side on which MASCOT is lying when at rest. To fulfill these tasks the GNC system consists of two types of sensors distributed over the MASCOT body as well as onboard algorithms running on the MASCOT onboard computer as part of the onboard software.

The algorithm to detect the motion state (free fall, in proximity, at rest) is a decision logic which in principal checks if the sensor readings are not changing for a specific amount of time. The algorithm for the estimation of the side on which MASCOT is lying is explained in detail in section 3.

The sensors used in the MASCOT GNC system are Optical Proximity Sensors (OPS) and Photoelectric Cell sensors (PEC).

OPTICAL PROXIMITY SENSOR (OPS)

The OPS, designed and manufactured by *cosine measurement systems*, is a small sensor (32.6 mm × 27 mm × 21.6 mm) with a mass of about 28 g. It consists of an infrared LED and an appropriate photo-diode (see Fig. 3). The light omitted by the LED is reflected by any object in the Field of View (FoV) of the sensor. Nearer objects reflect more light and light from objects further away than 12 cm can not detected any more. This gives the opportunity to detect objects in proximity in a certain direction. In addition the LED is on/off modulated by the OBC and the signal from the photo-diode is correlated with this modulation. With this method one can distinguish between reflected light from the LED and background illumination e.g. from sunlight. Fig. 4 shows the output voltage of the OPS as function of the distance from the object.
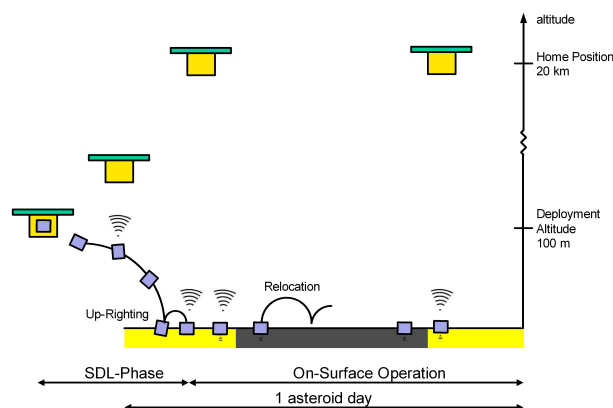

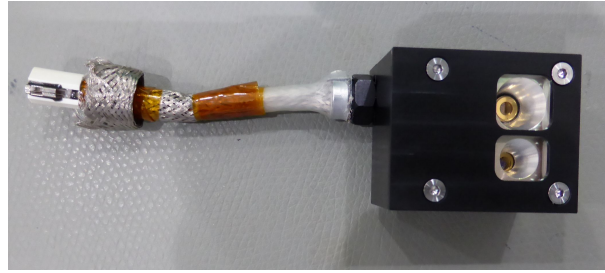***Fig. 2:*** *Sketch of Separation & surface operation concept*
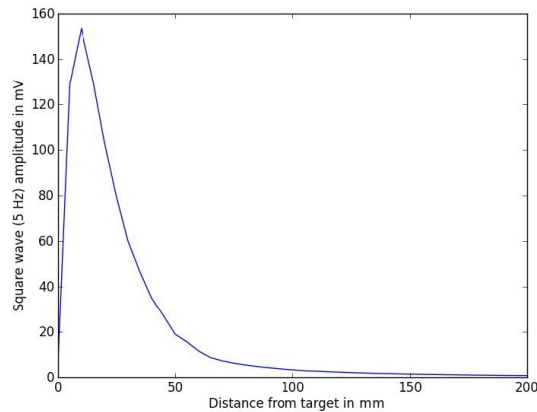
Fig. 3: Optical Proximity Sensor (OPS)

Fig. 4: OPS output voltage as function of distance

Five of these sensors are used on MASCOT, mounted on 5 different sides of the cuboid. Only the instrument side is not equipped with such a sensor. This space is needed for the scientific instruments. As one can see in Fig. 4 the output voltage decreases again for distances smaller than 10 mm. To prevent such small distances, the sensors are not mounted flat to the surface but shifted inside the body of MASCOT.

The sensors have been built by cosine Research B.V. [3].

PHOTOELECTRIC CELL SENSOR (PEC)

The PEC is a solar cell based sun sensor. It holds a space qualified triple junction solar cell (measuring 20 mm × 20 mm) on a 20.5 mm × 45 mm PCB together with two 50 Ω resistors connected in parallel to the solar cell (see Fig. 5). Due to Lambert's cosine law the output voltage U_{PEC} is proportional to the cosine of the angle ϕ between the sun vector $\underline{v}_{Sun}$ and the normal vector of the solar cell $\underline{n}_{PEC}$:

$$U_{PEC} = U_0 \cos \phi = U_0 \frac{\underline{v}_{Sun} \cdot \underline{n}_{PEC}}{|\underline{v}_{Sun}||\underline{n}_{PEC}|}. \tag{1}$$

Six of these sensors are used on MASCOT, one on every side of the MASCOT body. This makes it possible to measure the sun vector in body fixed frame in all possible directions.

The sensors have been built by ZARM Technik AG, Bremen [7].

For the OPS as well as the PEC windows have been cut out in the outer wall of MASCOT (see Fig. 6).

3. HISTOGRAM FILTER FOR ATTITUDE DETERMINATION

For MASCOT, the state that has to be determined is the side of the MASCOT cuboid on which the lander is lying. In other words the side which faces the soil. If MASCOT is tilted, e.g. because the terrain is not flat, the side
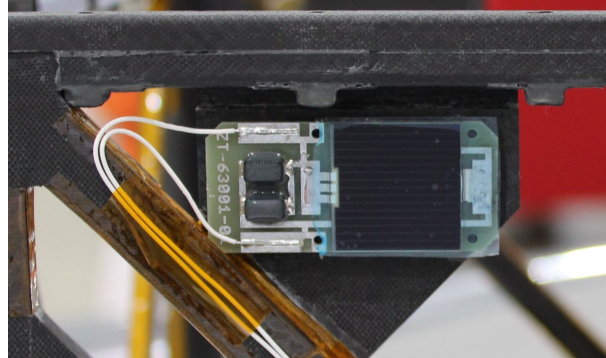
4

Fig. 5: Photoelectric Cell Sensor (PEC) glued to MASCOT structure

Fig. 6: MASCOT (bottom view) with separation mechanism and windows for GNC sensors

which faces the soil the most needs to be determined. Tilted and non-tilted orientations are combined to one discrete state instance. So the state space is discrete and can be divided in a finite number of states. For this application the number of states is $N_s = 6$. For this types of system a so-called histogram (or grid-based Bayesian) filter can be used.

A. BAYESIAN FILTERS

Given the time-discrete dynamics function of a system by

$$\underline{x}_k = \underline{f}_k(\underline{x}_{k-1}, \underline{v}_{k-1}) \tag{2}$$

with $\underline{f}$ as a possibly nonlinear function of the state $\underline{x}$ and the process noise $\underline{v}$. The measurement function is given by

$$\underline{z}_k = \underline{h}_k(\underline{x}_k, \underline{n}_k) \tag{3}$$

with the possibly nonlinear function $\underline{h}$ of the state and of the measurement noise $\underline{n}_k$. The objective of any estimation filter is to recursively estimate the state $\underline{x}_k$ from all available measurements $\underline{z}_{1:k}$ up to time k.

A Bayesian filter recursively calculates the probability density function (PDF) $p(\underline{x}_k | \underline{z}_{1:k})$. Assumed the initial PDF $p(\underline{x}_0)$ is known, the PDF $p(\underline{x}_k | \underline{z}_{1:k})$ can be obtained in two stages: prediction and update.

If the PDF $p(\underline{x}_{k-1} | \underline{z}_{1:k-1})$ at time $k-1$ is available, the predicted PDF can be obtained using the system dynamics (2):

$$p(\underline{x}_k | \underline{z}_{1:k-1}) = \int p(\underline{x}_k | \underline{x}_{k-1}) p(\underline{x}_{k-1} | \underline{z}_{1:k-1}) d\underline{x}_{k-1}. \tag{4}$$

The probabilistic model of the state evolution $p(\underline{x}_k | \underline{x}_{k-1})$ is defined by the system dynamics (2) and the statistics of the process noise $\underline{v}_{k-1}$.

The measurement update of the PDF is given using Bayes' rule

$$p(\underline{x}_k | \underline{z}_{1:k}) = \frac{p(\underline{z}_k | \underline{x}_k) p(\underline{x}_k | \underline{z}_{1:k-1})}{p(\underline{z}_k | \underline{z}_{1:k-1})} \tag{5}$$

with the normalizing constant

$$p(\underline{z}_k | \underline{z}_{1:k-1}) = \int p(\underline{z}_k | \underline{x}_k) p(\underline{x}_k | \underline{z}_{1:k-1}) d\underline{x}_k. \tag{6}$$

The PDF $p(\underline{z}_k | \underline{x}_k)$ depends on the measurement model (3) and the statistics of the measurement noise $\underline{n}_k$.

Equations (4) and (5) can be used to recursively compute the PDF $p(\underline{x}_k | \underline{z}_{1:k})$ at each time step. Of course this can not be done analytically in general. For certain assumptions solutions exist:

- Kalman Filter: The system is linear and the noise is Gaussian distributed.

- Histogram Filter/Grid-Based Filter: The state space is discrete and can be divided in a finite number of states.

Other filters approximate the optimal Bayesian solution, e.g. Extended Kalman Filter or Particle Filters [1] [2].

B. HISTOGRAM FILTERS/GRID-BASED FILTERS

If the state space is discrete and consists of a finite number of states, the Histogram Filter (or Grid-Based Filter) provides the optimal solution for the estimation of the PDF $p(\underline{x}_k | \underline{z}_{1:k})$ [1] [8]. Let the finite number of

states be N_s. For each state $\underline{x}_k^i, i = 1, \ldots, N_s$ at time k, let the conditional probability be $p_{k|k}^i$. Then the PDFs can be written using the Dirac function $\delta()$:

$$p(\underline{x}_{k-1}|\underline{z}_{1:k-1}) = \sum_{i=1}^{N_s} p_{k-1|k-1}^i \delta\left(\underline{x}_{k-1} - \underline{x}_{k-1}^i\right) \tag{7}$$

$$p(\underline{x}_k|\underline{z}_{1:k-1}) = \sum_{i=1}^{N_s} p_{k|k-1}^i \delta\left(\underline{x}_k - \underline{x}_k^i\right) \tag{8}$$

$$p(\underline{x}_k|\underline{z}_{1:k}) = \sum_{i=1}^{N_s} p_{k|k}^i \delta\left(\underline{x}_k - \underline{x}_k^i\right). \tag{9}$$

With this, the prediction and update equation can be written as

$$p_{k|k-1}^i = \sum_{j=1}^{N_s} p_{k-1|k-1}^j p(\underline{x}_k^i|\underline{x}_{k-1}^j) \tag{10}$$

$$p_{k|k}^i = \frac{p_{k|k-1}^i p(\underline{z}_k|\underline{x}_k^i)}{\sum_{j=1}^{N_s} p_{k|k-1}^j p(\underline{z}_k|\underline{x}_k^j)}. \tag{11}$$

If the transition probability $p(\underline{x}_k^i|\underline{x}_{k-1}^j)$ does not depend on time t nor on any external input u, it can be interpreted as elements of a constant transition matrix $\underline{P}_{k|k-1}$. With this, the prediction equation (10) can be written as a linear matrix equation:

$$\underline{p}_{k|k-1} = \underline{P}_{k|k-1}\underline{p}_{k-1|k-1}. \tag{12}$$

This linear equation can be understood as a system model acting on the discrete probability distribution $\underline{p}$ instead of the state vector $\underline{x}$. Using the law of total probability and Bayes' theorem one can also prove that

$$\sum_{i=1}^{N_s} p(\underline{x}_k^i|\underline{x}_{k-1}^j) = 1. \tag{13}$$

That means that the sum of all elements of one column of the matrix $\underline{P}$ is 1.

Looking at the update equation (11) one can see that the normalizing factor $\sum_{j=1}^{N_s} p_{k|k-1}^j p(\underline{z}_k|\underline{x}_k^j)$ in the denominator is the same for all possible state $\underline{x}_k^i$. That means that this factor doesn't have to be computed explicitly. Instead, it is also possible to scale the $p_{k|k}^i$ such that $\sum_i p_{k|k}^i = 1$.

If there are several measurements it is even easier to split the measurement vector $\underline{z}$ into several scalar measurements z^l and define the conditional probability $p(z_k^l|\underline{x}_k^i)$ for each of them. In that case (11) has to be applied sequentially.

If one wants to apply the Histogram Filter to a system two things have to be done:

- Define the transition matrix $\underline{P}_{k|k-1} = \left[p(\underline{x}_k^i|\underline{x}_{k-1}^j)\right]$.

- Define the continuous PDF $p(z_k^l|\underline{x}_k^i)$ for each measurement z^l and each possible state $\underline{x}^i$.

C. HISTOGRAM FILTER FOR MASCOT GNC

As already stated at the beginning of the section the task of the MASCOT GNC system is to determine the side of the MASCOT cuboid on which it is lying. Due to this fact the number of possible states is $N_s = 6$. The probability vector $\underline{p}$ is defined as

$$\underline{p} = \begin{pmatrix} p(x = x^1) \\ \vdots \\ p(x = x^6) \end{pmatrix} = \begin{pmatrix} p(\text{MASCOT is lying on side 1}) \\ \vdots \\ p(\text{MASCOT is lying on side 6}) \end{pmatrix}. \tag{14}$$

PREDICTION

The first step to be done to apply the Histogram Filter to the MASCOT GNC system is to define the probability transition matrix $\underline{P}_{k|k-1}$. Each element of this matrix represents the probability to flip from one side to another. The probability that MASCOT keeps lying on the same side as in the previous time step is denoted t, while the probability of changing to an adjacent side will be called q. s is the probability of switching to the opposite side. Due to (13) it holds that

$$t + 4q + s = 1. \tag{15}$$

The complete probability transition matrix $\underline{P}$ can than be written as

$$\underline{P}_{k|k-1} = \begin{pmatrix} t & q & s & q & q & q \\ q & t & q & s & q & q \\ s & q & t & q & q & q \\ q & s & q & t & q & q \\ q & q & q & q & t & s \\ q & q & q & q & s & t \end{pmatrix} \tag{16}$$

The numbering of the sides of MASCOT can be seen in Fig. The values of t, q and s depend on the dynamics (especially on the attitude rate) of MASCOT as well as on the sample time $\Delta t = t_k - t_{k-1}$. Setting them to constant values is of course a very rough simplification of the reality. The real dynamics of MASCOT while rolling and hopping over the asteroids surface depend on:

- Structural properties of MASCOT lander

- Unknown soil parameters of asteroid surface

- Unknown terrain geometry.

Even with known soil parameters and terrain geometry it is hard to simulate the contact dynamics between the MASCOT body and the asteroid surface. Unknown soil parameters and terrain geometry makes it impossible to find a realistic dynamic model which can be implemented onboard the lander. This is why the simplified dynamic model (16) will be used. For this model, the following assumptions have been made:

- Transition probabilities t, q and s are the same for all sides of MASCOT.

- Transition probabilities don't depend on attitude rate, i.e. they are constant over time.

For a short GNC sample time of 2 s the transition probabilities have been set according to the following table:

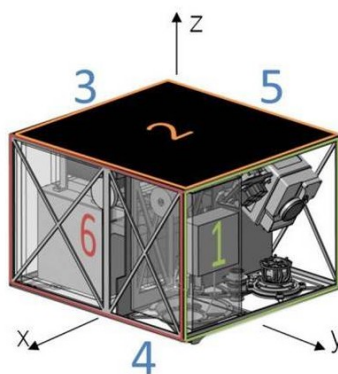| t	q	s
0.89	0.028	0

Fig. 7: MASCOT side numbering

UPDATE

For the update, a PDF $p(z^l|x^i)$ has to be defined for each measurement z^l and each possible state x^i. Please note that the update will be performed sequentially and such all the measurements z^l are scalar. Also the state x is a scalar in our case. The PDF $p(z^l|x^i)$ is specific for each measurement and each possible state and depends continuously on the measurement z^l.

OPS update   In the case of the Optical Proximity Sensor (OPS) there are 5 measurements and 6 possible states. So the number of PDFs to be defined is $5 \times 6 = 30$. But there are only two types of PDFs: If the sensor is mounted on the appropriate side of MASCOT, the contact-PDF p_{CO} is used. Otherwise, the non-contact-PDF p_{NC} is used. The PDF type used for each OPS and each side of MASCOT is given in Table 1. It can also be seen that on side No. 4 (the instrument side) no OPS is mounted and so no PDF of type CO will be used.

The PDF $p_{CO}(z)$ defines the probability density of a measurement z given that the appropriate side of MASCOT is the bottom side and thus the appropriate OPS measures a contact to the soil. In this case it is very unlikely that the output of the sensor is almost zero. Other values are possible, depending on how rough the surface of the asteroid is and how flat MASCOT is lying on it. But larger output values (smaller distance to ground) are more likely than smaller ones (larger distance to ground, see Fig. 4). Thus the probability increases up to a value of about 1.2 V. This is reflected in the PDF $p_{CO}(z)$ shown in Fig. 8. The plot only shows a cutout of the complete PDF which stays constant for larger measurement values up to the maximum measurement value of 5 V. Note that, due to the law of total probability,

$$\int_{-\infty}^{\infty} p(z^l|x^i)dz^l = 1 \ \forall z^l, x^i. \tag{17}$$

The PDF $p_{NC}(z)$ reflects the probability of a measurement z in the case that the side of MASCOT has no contact to the soil and thus the appropriate OPS doesn't see any object in proximity. The expected output of the OPS is 0 V plus the noise of the sensor. So the probability density for values $\leq 20\,\text{mV}$ is large, while for values $\geq 30\,\text{mV}$ it is almost zero. The PDF $p_{NC}(z)$ is also shown in Fig. 8. Note that there is no value z for which any of the two types of PDFs is set to 0. This is to reflect failure cases, which are unlikely but not impossible.

In the onboard software, the PDFs for the OPS are implemented as lookup tables with linear interpolation between the data points.

PEC update   From the characteristic curve of the PECs (eq. 1) one can show that

$$\sum_{i=1}^{6} U_{PEC,i}^2 = U_0^2. \tag{18}$$

This makes it easy to normalize the PEC measurement by U_0 which depends on the solar radiation:

$$\hat{U}_{PEC,i} = \frac{U_{PEC,i}}{\sqrt{\sum_{i=1}^{6} U_{PEC,i}^2}} = \cos\phi_i. \tag{19}$$

Table 1: Measurement PDFs for OPS

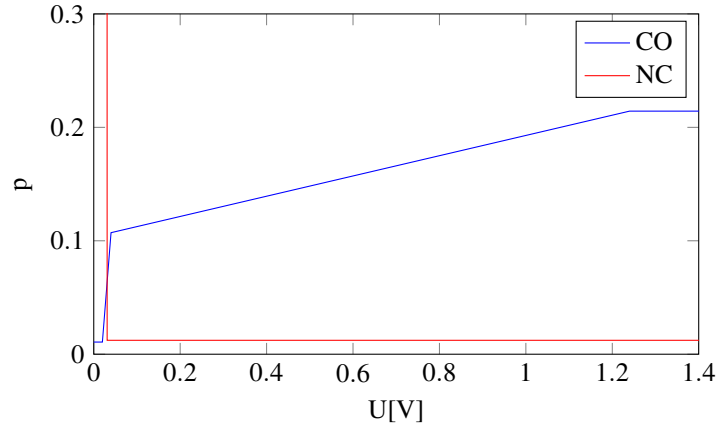|		OPS-No.				
		1	2	3	4	5
	1	NC	**CO**	NC	NC	NC
	2	NC	NC	NC	NC	**CO**
	3	NC	NC	NC	**CO**	NC
Side-No.	4	NC	NC	NC	NC	NC
	5	NC	NC	**CO**	NC	NC
	6	**CO**	NC	NC	NC	NC

9

Fig. 8: Contact (CO) and non-contact (NC) PDF of OPS (cutout)

For the PEC $6 \times 6 = 36$ PDFs $p(z^l|x^i)$ are needed, but again only 3 types of PDFs are used. For each possible side of MASCOT the following PDFs are defined:

- **Bottom** (BT) This PDF is used for the measurement of the PEC which is mounted on the appropriate side. Thus it is facing the asteroid and does not see the sun. The expected output is $\mu_{BT} = 0\,\text{V}$.

- **Top** (TP) This PDF is used for the measurement of the PEC which is mounted opposite to the appropriate side. The expected output depends on the elevation of the sun ε above the local horizon:

$$\mu_{TP} = \text{E}\left(\text{acos}\,\hat{U}_{PEC,TP}\right) = \text{E}\left(\phi_{TP}\right) = 90° - \varepsilon. \tag{20}$$

  Note that the measurement $\hat{U}_{PEC,TP}$ has been transformed to angle space by applying the arccosine.

- **RSSS** (Root sum of squared sides) It is known that the summed square of the normalized measurements from all 6 PECs is 1. If one combines all the measurements from the PEC which are neither on the top nor on the bottom by summing up the squared values it holds that

$$\mu_{RSSS} = \text{E}\left(\text{acos}\,\sqrt{\sum_{sides} \hat{U}_{PEC,i}^2}\right) = \text{E}\left(\text{acos}\,\sqrt{1 - \hat{U}_{PEC,TP}^2}\right) = \text{E}\left(\text{asin}\,\hat{U}_{PEC,TP}\right) = \varepsilon. \tag{21}$$

As PDFs normal distributions are used with the defined expected values and user-definable variances σ^2. The standard deviations are set to

σ_{TP}	σ_{RSSS}	σ_{BT}
15°	15°	0.15

The corresponding PDFs for a sun elevation of 55° are shown in Fig. 9. As the equation for the PDF of a normal distribution is known, the value of the PDF in the onboard software can be computed from the measurements and the sun elevation without using a lookup table.

4. TEST AND VERIFICATION

A. SIMULATION

To develop and verify the MASCOT GNC onboard algorithms, a MATLAB/SIMULINK simulation has been developed. The simulation consists of the following parts:

- Simple trajectory generator using an arbitrary terrain model
- Sensor models including sun elevation and line of sight computation
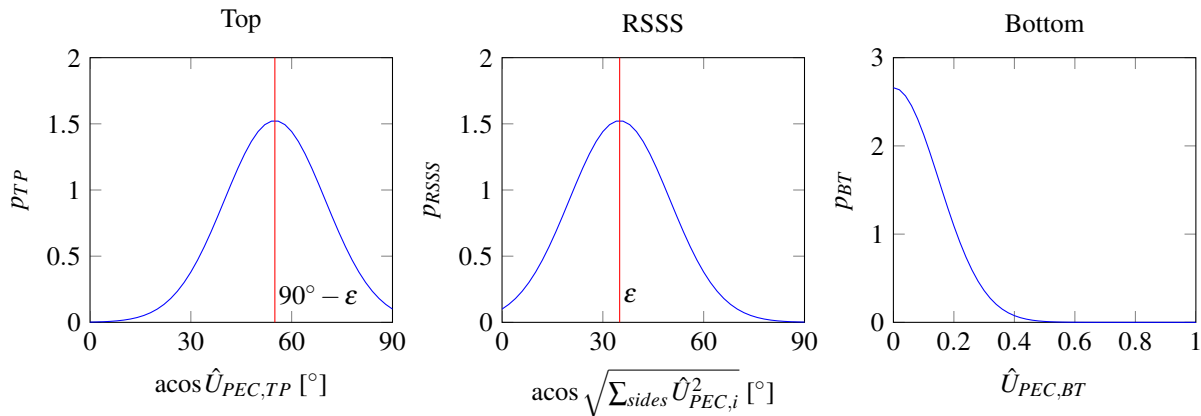
Fig. 9: *Top, bottom and RSSS PDF of PEC for a sun elevation of* $55°$

- Onboard algorithms

- Analysis tools

TRAJECTORY GENERATOR

A simple trajectory generator has been developed. The contact dynamics has been modeled as a mass-spring-damper system and such it is not realistic. But due to the simple model the generator can be processed very fast which gives us the possibility to run Monte-Carlo simulations. The parameters of the model has been adjusted to produce realistic velocities, attitude rates and times in which MASCOT comes to rest. The trajectory generator also produces realistic resting positions. For that the altitude of each edge of MASCOT relative to the terrain model is computed. If the altitude is negative an upward force depending on relative altitude and velocity acts on the body of MASCOT. This force also causes a torque depending on the lever arm between the edge and the center of gravity. In addition, the gravitational force of the asteroid also acts on the body of MASCOT. These forces and torques are the input for the well-known dynamic differential equations.

In addition a multibody simulation with a complex soil model has been built to produce more realistic trajectories. For this a dedicated multibody simulation tool has been used. Due to a large computational effort this simulation is not suitable for Monte-Carlo simulations. But the resulting trajectories can be fed in the MASCOT GNC simulation to test the behavior of the GNC system for specific trajectories.

The terrain model used in the MASCOT GNC simulation is based on regular grid points at which arbitrary elevations can be defined. This gives the possibility to define terrains with varying steepness and roughness.

SENSOR MODELS

Using the trajectory (position, attitude) from the trajectory generator as well as the terrain model, the line of sight of each OPS can be computed (see Fig. 10). The terrain model is the same as the one used be the trajectory generator. Knowing the distance to voltage relation (see Fig. 4) the output of each OPS can be computed. The sensor model also includes noise and the possibility to simulate sensor failures.

SIMULATION RESULTS

The following figures show an example trajectory, the appropriate sensor output voltages as well as the result of the attitude estimation. In Fig. 11 one can see the altitude of the MASCOT center, the rotation around the x-axis α and the rotation around the y-axis β. The simulation starts at an altitude of $10\,\text{m}$ with random velocity, attitude and attitude rate. At about $t = 160\,\text{s}$ MASCOT touches the asteroid
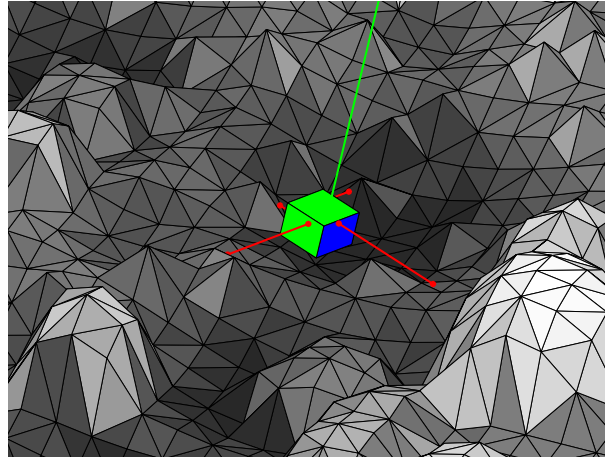
Fig. 10: *MASCOT in resting position on rough terrain, lines of sight of OPS plotted*

surface for the first time. This changes the attitude rate and MASCOT is rolling over the surface until it comes to rest at about $t = 750\,\mathrm{s}$. As the angle α is at about $180°$ at the end of the simulation, MASCOT comes to rest lying on his back. In Fig. 12 the output voltages of the different sensors are shown.

The probabilities of the each surface is plotted in Fig. 13, depending only on OPS, only on PEC and the combination of both. One can see that probabilities computed from OPS and from PEC estimate the same "'side to soil'" for the most times, but not always. This is because the OPS also detects a nearby surface if this surface is left or right from MASCOT. On the other hand the PECs can not provide a non-ambiguous estimation if the sun elevation is low.

The last figure (Fig. 14) shows the result of the attitude estimation. On the left plot one can see the total PDF including propagation. The center plot shows the estimated (most likely) side to soil together with the true side to soil. For most times the estimated value coincides with the true value with a delay, which is caused by the propagation. the most important thing is that the estimated and the true value are the same when MASCOT comes to rest. The estimated status of the lander has been plotted in the right figure.

B. MONTE-CARLO SIMULATIONS

It is planned to do Monte-Carlo simulations using the described software simulator. Including trajectories from the more realistic multibody simulation gives us the possibility to adapt parameters of attitude determination algorithm, especially the values for probability transition matrix $\underline{P}$ and for the measurement PDFs $p(z^t|x^t)$. Varying the roughness of the terrain will show up to which roughness the GNC system will
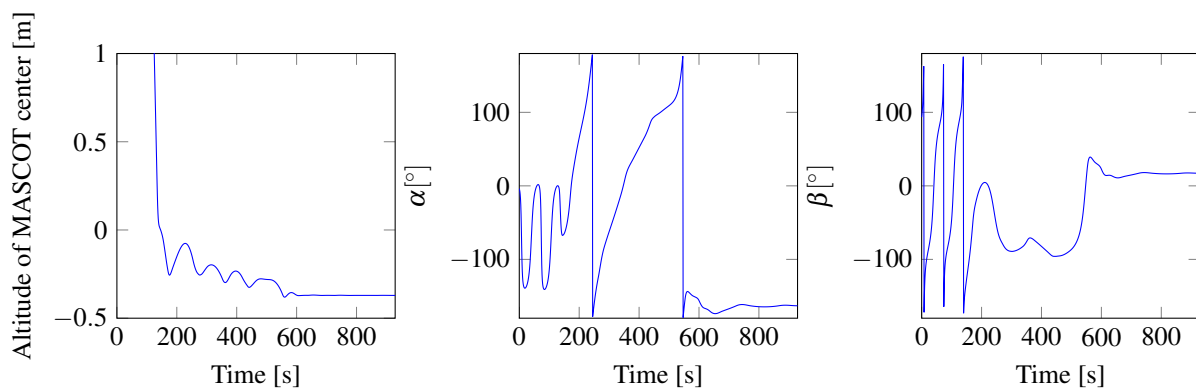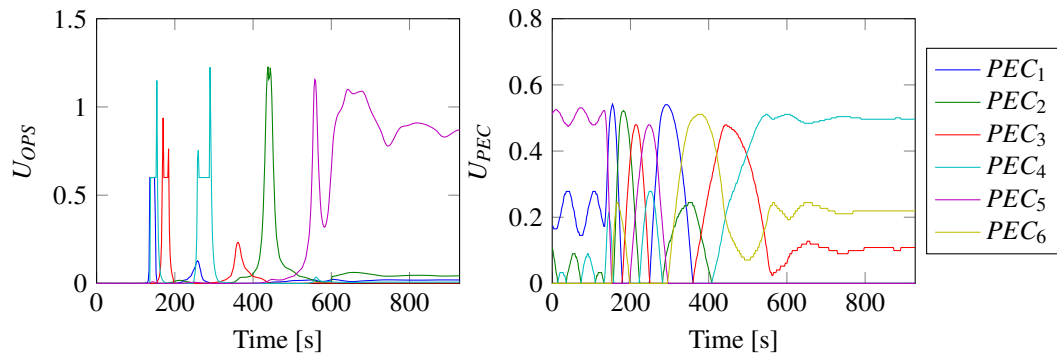

Fig. 11: *Simulated sample trajectory*

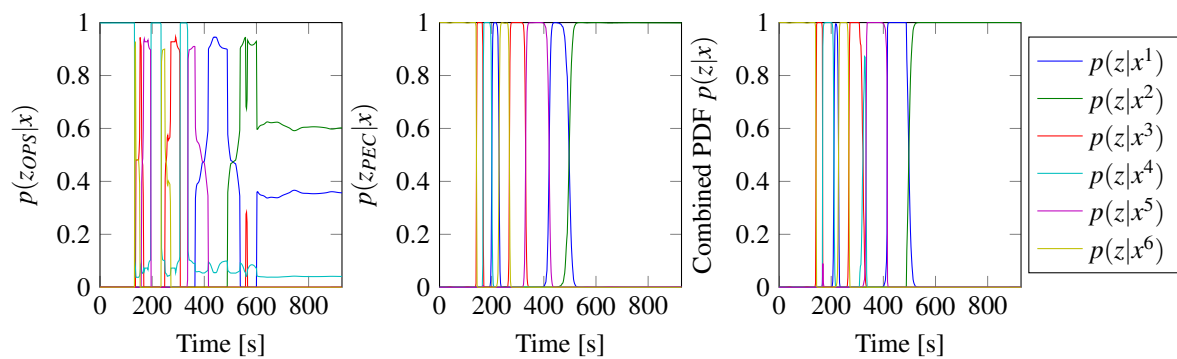*Fig. 12: Output voltage of OPS and PEC*
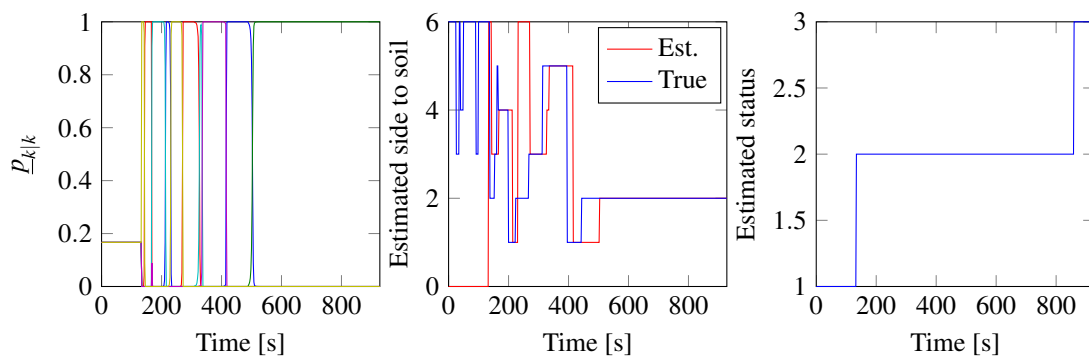

Fig. 13: Measurement PDF

Fig. 14: Total PDF, estimated side to soil and status (1 = free fall, 2 = moving in proximity of asteroid, 3 = at rest)

work reliably and when it will start to estimate the wrong side to soil due to large nearby stones. This will also influence the landing site selection at the asteroid.

C. SOFTWARE DEVELOPMENT AND VALIDATION FACILITY

A Software Development and Validation Facility (SDVF) based on the ESA SIMSAT simulation environment has been built for MASCOT. It contains simulation models for MASCOT subsystems as well as interfaces to the real hardware. It also allows the usage of an emulator of the selected LEON chip instead of the real processor hardware.

In the context of the GNC subsystem, the SDVF allows Hardware-In-The-Loop (HIL) testing of the GNC subsystem in the loop with the mobility subsystem, the MASCOT Autonomy Manager (MAM) and simulated dynamics of MASCOT. Again, it is not possible to run the complete multibody simulation of the MASCOT dynamics on the SDVF. Such, the modeling approach is based on a finite number of precalculated trajectory parts. Each trajectory part starts and ends with MASCOT lying on one of the 6 possible sides, except the free fall trajectory parts which start with the separation from the mother ship. When being at rest, the next trajectory part is chosen depending on the attitude estimation of the GNC system, the decision of the autonomy manager and the actuation from the mobility system. This gives the possibility to simulate a complete MASCOT mission starting from the separation from the mother ship until the battery is empty.

The GNC sensor models are the same as the ones for the pure software simulation of the GNC system (see section 4.A). The GNC algorithms are part of the onboard software and as such run on the real processor hardware or on the emulator.

D. MASCOT GNC MOCKUP

A mockup of the MASCOT structure including the engineering models of the GNC sensors has been built to test the GNC subsystem in a realistic environment (see Fig. 15). It is planned to let the mockup drop on a terrain model with expected roughness and albedo, while the PEC will be stimulated by the Sun. To get a realistic free fall velocity and attitude rate while rolling on the asteroid, the mockup will be suspended by a string. During the movement, the data from the OPS as well as the PEC will be sampled by a USB measurement card and recorded for later use. This data can be fed into the MATLAB/SIMULINK simulation of the GNC algorithms to test the correct function of the attitude estimation algorithm. This test setup gives us the possibility to fed the onboard algorithms with real sensor data. Of course, only a limited number of test trajectories are possible.
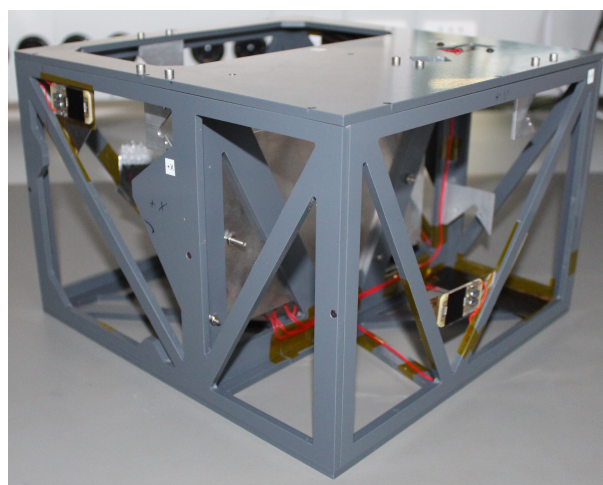

Fig. 15: MASCOT Mockup including GNC sensors

5. CONCLUSION

The small asteroid lander MASCOT imposes specific requirements in its GNC system. A Histogram Filter has been proposed as central algorithm for sensor data fusion and attitude estimation. The theory behind this filter has been shown as well as how it can be adapted to the needs and the GNC sensors of MASCOT. A software simulation has been built to verify the behavior of the filter and the fulfillment of the requirements and simulation results have been shown.

In the next steps the GNC system has to proof its performance in Monte-Carlo simulations, varying initial conditions, sun elevation and terrain roughness. Furthermore Hardware-In-The-Loop tests will be conducted together with other subsystems of MASCOT.

REFERENCES

[1] Sanjeev Arulampalam, Simon Maskell, Neil Gordon, and Tim Clapp. A Tutorial on Particle Filters for On-line Non-linear/Non-Gaussian Bayesian Tracking. *IEEE Transactions on Signal Processing*, 50:174–188, 2001.

[2] Zhe Chen. Bayesian filtering: From Kalman filters to particle filters, and beyond. *Statistics*, 182(1):1–69, 2003.

[3] S. Conticello, P. F. Manzillo, and M. Esposito. MASCOT GNC sensor system, Detailed design. Design report CR-MGNC2-TN03, cosine Research B.V., March 2014. Internal document.

[4] J. Côté, A. Kron, J. de Lafontaine, J. Naudet, and S. Santandrea. PROBA-2 Attitude and Orbit Control System: In-Flight Results of AOCS Flight Experiments. In *8th International ESA Conference on Guidance, Navigation & Control Systems*. European Space Agency, 2011.

[5] Zhuohua Duan, Zixing Cai, and Jinxia Yu. Adaptive Particle Filter for Unknown Fault Detection of Wheeled Mobile Robots. In *Intelligent Robots and Systems, 2006 IEEE/RSJ International Conference on*, pages 1312–1315, Oct 2006.

[6] Josef Reill, Hans-Jürgen Sedlmayr, Sebastian Kuß, Philipp Neugebauer, Maximilian Maier, Andreas Gibbesch, Bernd Schäfer, and Alin Albu-Schaeffer. Development of a Mobility Drive Unit for Low Gravity Planetary Body Exploration. In *ASTRA - 12th ESA Symposium on Advanced Space Technologies for Robotics and Automation*, 2013.

[7] M. Rossol and A. Schotten. DLR Solar Cell Systems, Angle Dependant Solar Cell Measurement. Test report DLR-TR-ZAR-SCS-01, ZARM Technik AG, September 2013. Internal document.

[8] Sebastian Thrun, Wolfram Burgard, and Dieter Fox. *Probabilistic Robotics*. Intelligent robotics and autonomous agents series. The MIT Press, 2005.

[9] L. Witte, J. Biele, A. Braukhane, Florian Herrmann, T.-M. Ho, C. Krause, Sebastian Kuß, C. Lange, M. Schlotterer, S. Ulamec, and S. Wagenbach. The Mobile Asteroid Surface Scout (MASCOT) - System & Mission Engineering and Surface Operations Concept. In *Global Space Exploration Conference - GLEX*, April 2012.

[10] C. Ziach, J.-P. Bibring, J. Biele, M. Deleuze, R. Findlay, T.-M. Ho, R. Jaumann, C. Lange, T. Okada, S. Ulamec, L. Witte, and H. Yano. The final development stages of MASCOT, a small asteroid lander to accompany Hayabusa-II. In *64th International Astronautical Congress*, September 2013.